Title:

Dynamic Wt1 expression in the gastrulation-stage mouse embryo specifies vascular and visceral smooth muscle cell fate independently from mesothelial fate.

Authors: Suad H. Alsukari[1,3], Huei Teng Ng[1], Lilly Lang[1], Sharna Lunn[2], Shanthi Beglinger[1], Lauren Carr[1], Michael Boyes[1], David A. Turner[2] and Bettina Wilm[1]*

Affiliations:

[1]Department of Women's and Children's Health, Institute of Life Course and Medical Sciences, Faculty of Health and Life Sciences, University of Liverpool, Liverpool, UK

[2]Department of Musculoskeletal and Ageing Science, Institute of Life Course and Medical Sciences, Faculty of Health and Life Sciences, University of Liverpool, Liverpool, UK

[3]current address: Department of Biology, Albaha University, Albaha, KSA

*To whom correspondence is to be addressed (bwilm@liverpool.ac.uk)

Acknowledgements:

We acknowledge funding by the BBSRC Alert13, grant number BB/L014947/1, for the Zeiss Z.1 Light sheet microscope. We are also indebted to the University of Liverpool's (UoL) Centre for Cell Imaging (CCI) facility for provision of state-of-the-art imaging equipment funded through grants awarded to the University of Liverpool's CCI by the MRC (MR/K015931/1) and the BBSRC (BB/M012441/1, BB/R01390X/1), and for excellent technical support, assistance, and training. We express our thanks to the Biomedical Services Unit at the University of Liverpool, for expert support in mouse maintenance, breeding and timed mating. We acknowledge Sumaya Dauleh and Thomas P. Wilm for technical assistance.

Author Contributions: BW conceived and designed the study. SHA, HTN, LL, SL, SB, LC, MB, DAT and BW performed experiments and analysed the data. HTN analysed the scRNAseq datasets and interpreted it with DAT and BW. DAT and BW wrote the manuscript

with input from HTN and SHA. All authors discussed the results and commented on the manuscript.

Funding:

BW was supported by MRC project grant MR/M012751/1 and the BBSRC Doctoral Training Partnership scheme (BB/M011186/1 for MB; BB/T008695/1 for HTN), and acknowledges generous funding from the Albaha University, Saudi Arabia (PhD Studentship to SHA). SB was funded by an NHS Student Bursary. LL and LC were MRes students self-funding their studies. DAT was supported in this work by a BBSRC New Investigator Grant (BB/X000907/1; SL) and a David Sainsbury NC3Rs Fellowship (NC/P001467/1).

1. Abstract

The Wilms' Tumour protein (Wt1) had previously been shown to specify both the mesothelial lineage and vascular smooth muscle cell (vSMC) lineage in the mouse intestine, with evidence suggesting that intestinal vSMCs arise from the mesothelium. Here, we dissect the temporal relationship between these two mesodermal lineages, reporting that unexpectedly, Wt1 expression already in gastrulation stage embryos specifies a population of SMC precursor cells in the lateral plate mesoderm (LPM). Tamoxifen-induced genetic lineage tracing of Wt1-expressing cells revealed that vSMC and visceral smooth muscle cells (visSMCs) of the foetal mid-gut are labelled when Tamoxifen was administered at E7.5 or E8.5. By contrast, intestinal mesothelial cells were labelled after Tamoxifen dosing from E9.5 and later. Analysis of scRNAseq data of gastrulation stage mouse embryos and confocal microscopy demonstrated for the first time Wt1 expression in epiblast and primitive streak, emerging mesoderm and, from E7.5 onwards, in the LPM. In E8.5 mouse embryos, the co-expression of key smooth muscle fate markers *Tagln*, *Acta2*, *MrtfA/B* and *Pdgfrb* in *Wt1*-expressing cells revealed that vSMC and visSMC fate is specified independently from visceral mesothelium formation. Together, our study provides insight into the developmental lineage of smooth muscle specified by Wt1 expression at gastrulation stages.

2. Introduction

The embryonic origin of vascular smooth muscle cells (vSMCs) is relatively diverse as different regions of the vasculature arise from different progenitors including neural crest cells (NCCs), lateral plate mesoderm (LPM) and somatic mesoderm [1]. Differentiation of vSMCs and tissue formation in vertebrates are driven by a series of canonical cell signalling events and mechanical forces which regulate progenitor cell recruitment, differentiation, and maturation [2-4]. Platelet derived growth factor receptor beta (Pdgfrb) signalling is a key regulatory pathway in vSMC myogenesis since disruption of Pdgfrb signalling reduces vSMC proliferation and recruitment [4,5]. Specification of vSMC is marked by expression of smooth muscle cell markers such as transgelin (Tagln), alpha-smooth muscle actin (Acta2), smooth muscle myosin heavy chain (Myh11), desmin and others [6,7]. However, the timepoint when these genes start to be expressed in embryonic development, and their roles during the early stages of vSMC specification and differentiation remain unclear.

Wilms' tumour protein 1 (Wt1) is a transcription factor involved in the development of several tissues and organs in normal embryogenesis. The earliest Wt1 expression was identified in the intermediate mesoderm (IM) and LPM in E9.5 mouse embryos [8]. Its most prominent roles are in the development of the kidneys, arising from the IM, and of the heart, where the Wt1-expressing epicardium contributes to coronary vessel formation [9,10]. The epicardium is the mesothelial layer of the heart, which is continuous with the pericardial mesothelium of the pericardial cavity. Wt1 is also expressed in the pleural and peritoneal mesothelium, lining the cavities and covering the organs housed within, from about E9.5 onwards and throughout adulthood [8,11-15].

Previously, studies showed that the epicardium can give rise to vSMC of the developing coronary vasculature [16,17]. Genetic lineage tracing experiments using a transgenic mouse line expressing Cre recombinase under control of regulatory elements of the human WT1 gene (*Tg(WT1-cre)AG11Dbdr*, in short: *Wt1-Cre*) in combination with the *Rosa*$^{LacZ/LacZ}$ reporter mouse revealed that a population Wt1-expressing serosa and pleural mesothelium cells give rise to vSMC in the peritoneal and lung cavity [13,15]. These results suggested that the mesothelium and vasculature of the intestine and lungs have a developmental relationship similar to that of the epicardium and the coronary vasculature. Similar studies using *mWt1/IRES/GFP-Cre* (*Wt1cre*) transgenic mice crossed with the *Rosa26R*^{EYFP} reporter mouse also found a contribution of Wt1-expressing mesothelial cells to the vasculature of the developing intestine [18].

93 In order to determine when mesothelial cells become committed to give rise to intestinal
94 vascular smooth muscle, we conducted pulse-chase studies of postnatal and adult mice
95 using a tamoxifen-inducible temporally-controlled and *Wt1*-driven Cre system
96 (*Wt1*$^{tm2(cre/ERT2)Wtp}$, *Wt1*^{CreERT2})[17]. Our results showed that Wt1-expressing peritoneal cells
97 maintained the mesothelium over the intestine and peritoneal wall (and contributed to
98 visceral fat, [19]), but failed to give rise to intestinal vasculature components. However, Wt1-
99 expressing epicardium was observed to contribute towards formation of coronary vessels
100 postnatally and in adult mice [14]. These findings suggested that the capacity of Wt1-
101 expressing mesothelial cells to differentiate into vSMCs must be restricted to developmental
102 stages.

103 We propose that there is an embryonic contribution of Wt1-expressing cells towards the
104 vSMC fate in the peritoneum and intestine, of which the temporo-spatial resolution and
105 molecular mechanisms have remained unresolved so far. Here, to address this, we used
106 the tamoxifen-inducible *Wt1*^{CreERT2} mouse line in combination with Rosa-based reporter mice
107 for lineage tracing analysis to determine the contribution of Wt1-expressing cells towards
108 intestinal vasculature in mouse embryo. Our results indicate that during embryonic
109 development, two distinct populations of Wt1-expressing cells emerge, one which defines
110 mesothelial cells from approximately E9.5 onwards, and one which defines SMC fate
111 predominantly at stages around E7.5 to E8.5. Lineage-traced cells were found not only as
112 vSMCs but also as visceral SMCs (visSMCs) in the intestinal wall. We provide, for the first
113 time, a detailed analysis of Wt1 expression in E6.5-E8.5 mouse embryos. *In silico* analysis
114 of single cell RNAseq data revealed that *Wt1* is co-expressed with the emerging mesoderm
115 marker *Brachyury* (*Bra*) and later with SMC markers in E6.5-E8.5 mouse embryos. We then
116 describe expression of Wt1 in the E7.5 and E8.5 mouse embryo in the primitive streak and
117 the emerging neuro-mesodermal progenitor cells using cutting edge confocal microscopy
118 techniques. Lastly, we show that Wt1-derived cells within the mesentery of the developing
119 intestine aligned with the developing endothelial vascular network and co-expressed Pdgfrb.
120 Together, these data reveal a novel developmental differentiation pathway of visceral and
121 vascular smooth muscle cells influenced by Wt1 expression and independent of
122 mesothelium formation.

123 ## 3. Results

124 **Contribution of *Wt1*-expressing cells to SMCs in the peritoneal cavity.**

125 To determine when during embryogenesis Wt1-expressing cells became fated to develop
126 into vSMCs, we combined the *Wt1*$^{CreERT2/+}$ lineage driver with either the *Rosa26R* (lacZ) or
127 the *Rosa26*^{mTmG} lineage reporter in mice, gave tamoxifen (Tam) once at different embryonic
128 stages (pulse), and performed endpoint analysis at stages around E18.5 (chase; see **Fig.**
129 **1A, Supplementary Fig. 1A** and **Supplementary Table 1**). We obtained similar results with
130 both reporter systems: Tam administration at E9.5 or up to E13.5, followed by endpoint
131 whole mount analysis, revealed almost exclusive labelling of mesothelial cells in the
132 mesentery and intestine at mid-intestinal level (**Fig. 1B-E**, **Supplementary Fig. 1C-F**,
133 **Supplementary Table 1**). When Tam was given to pregnant dams at E7.5 or E8.5 followed
134 by endpoint analysis, we observed instead labelled cells surrounding the developing vessels
135 of the mesentery, and in the visceral smooth muscle of the intestine at mid-intestinal level,
136 but barely in the mesothelium (**Fig. 1F-J**; **Supplementary Fig. 1G-K**). Littermates carrying
137 no *Wt1*^{CreERT2} allele showed no labelled cells (**Supplementary Fig. 1L, M**).

138 We also analysed the stomach and colon of foetuses under this experimental design, and
139 observed that Tam dosing at E7.5 resulted in labelling of visceral smooth muscle cells but
140 not mesothelial cells. By contrast, foetuses after Tam dosing at E8.5 showed a mixed
141 population of labelled cells in the stomach, mostly consisting of visceral smooth muscle; in
142 the colon, there were only labelled visceral smooth muscle cells. In foetuses which had
143 received Tam at E9.5 up to E14.5, cell labelling occurred predominantly in mesothelial cells
144 (**Supplementary Fig. 2**, **Supplementary Table 1**). However, after Tam dosing at E9.5 and
145 up to E11.5 we observed in a few foetuses occasional visceral smooth muscle cells that
146 were LacZ-positive, in the stomach and colon.

147 Interestingly, the spleen was not labelled when Tam was administered at E7.5, indicating
148 that Wt1 was not expressed yet at this stage in the cells that later will become splenic
149 precursors forming the putative splenic mesenchyme [20].

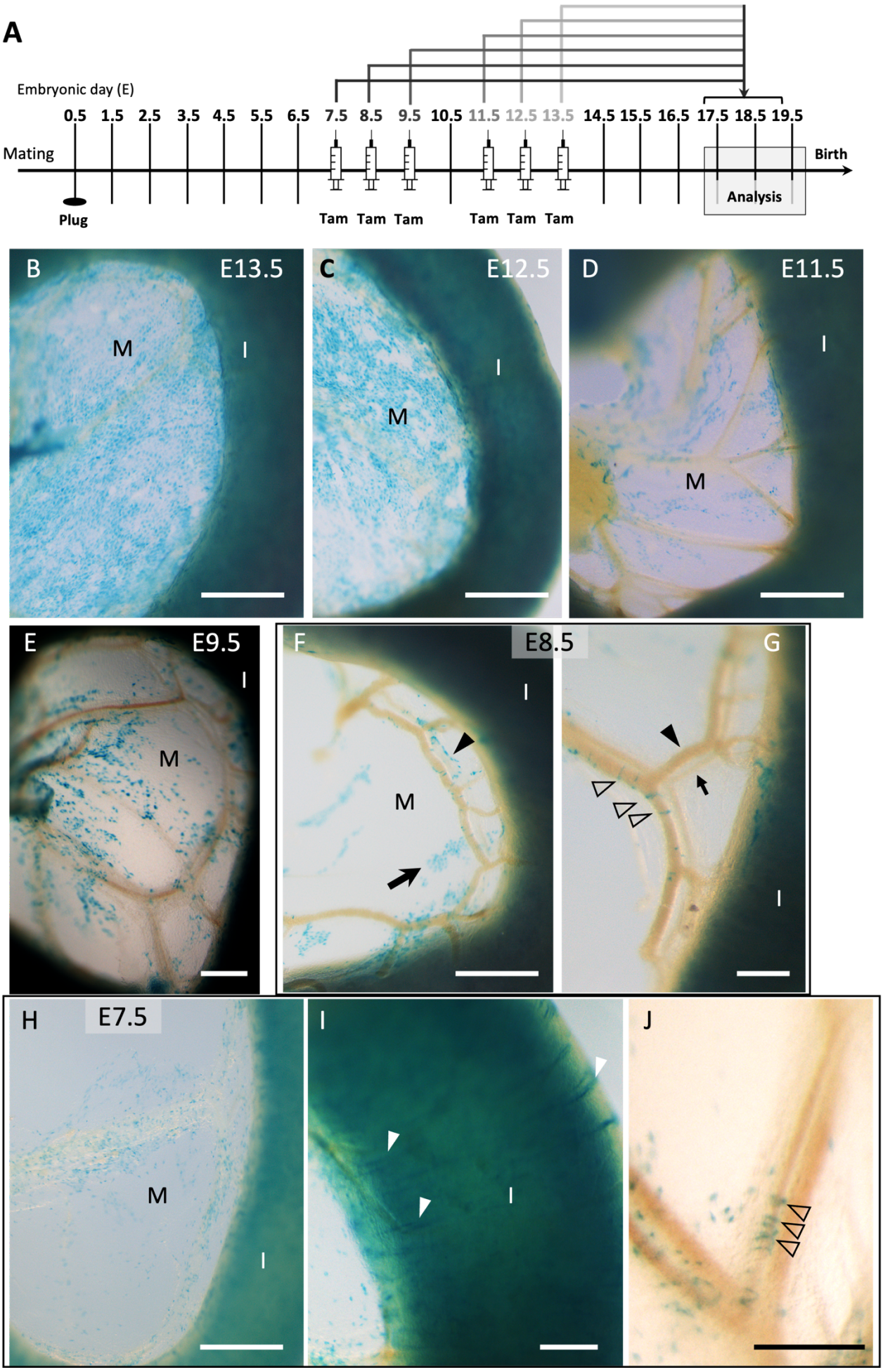
A
Embryonic day (E)
0.5 1.5 2.5 3.5 4.5 5.5 6.5 7.5 8.5 9.5 10.5 11.5 12.5 13.5 14.5 15.5 16.5 17.5 18.5 19.5
Mating
Plug
Tam Tam Tam
Tam Tam Tam
Analysis
Birth
B E13.5
M
I
C E12.5
M
I
D E11.5
M
I
E E9.5
M
I
F E8.5
M
I
G
I
H E7.5
M
I
I
I
J

Figure 1: Embryonic contribution of cells of the Wt1-lineage to visceral mesothelium or visceral and vascular smooth muscle is dependent on timing of tamoxifen dosing. A. Schematic of the study design: CD1 dams were time mated with *Wt1*$^{CreERT2/+}$;*Rosa26*$^{LacZ/LacZ}$ males and received tamoxifen (Tam) at the respective embryonic stages (embryonic day, E); embryos were dissected between E17.5 and E19.5, and XGal stained. **B.** When Tam was given at E13.5 and embryos analysed at E17.5, the mesentery (M) and intestine (I) were well covered by lacZ+ cells. **C, D.** When Tam had been given at E12.5, the coverage of LacZ-positive cells in the mesentery was less complete at E19.5. This loss of coverage with LacZ-positive cells was still more pronounced E17.5 when Tam had been given at E11.5 (D). **E.** Similarly, there were only patches of LacZ-positive cells in the mesentery and over the intestine at E17.5 after Tam administration at E9.5. **F, G.** When Tam had been given at E8.5, LacZ-positive cells were observed in small patches in the mesentery (arrow, F), or in cell chains near the vasculature (arrowhead, F), or in distinct rings (open arrowheads, G) surrounding the mesenteric veins (filled arrowhead, G) in the second arcade of the mesenteric vascular tree. The corresponding artery is depicted with an arrow (G). H-J. Tam dosing at E7.5 resulted at E18.5 in LacZ-positive cells scattered within the mesentery (H), in the circular musculature of the small intestine (white arrowheads, I), and surrounding a segment of mesenteric artery of the second arcade (black arrowheads, J). Scale bars, 500 µm (B, C, D, F, H), 200 µm (E, G, I, J).

Immunofluorescence staining on sections through intestine and mesentery of *Wt1*$^{CreERT2/+}$; *Rosa26*$^{mTmG/+}$ foetuses confirmed that after inducing Tam-based lineage tracing at E8.5, visSMCs and vSMCs co-expressed Acta2 and GFP and were found close to the CD31-positive vascular endothelial cells, while hardly any mesothelial cells (pan-cytokeratin, Wt1) were GFP-positive. By contrast, after Tam dosing at E11.5, mesothelial cells were GFP-labelled but no visSMCs or vSMCs (**Fig. 2**).

These results suggest that during embryonic development, two distinct populations of Wt1-expressing cells emerge, one which defines mesothelial cells from approximately E9.5 onwards, and one which defines visceral and vascular SMC fate predominantly at stages around E7.5 to E8.5.

An additional observation in the mice after Tam dosing at E7.5 and E8.5, was that labelled visSMCs and vSMCs could only be found in a short fragment of the mid-intestinal region including mesentery (**Supplementary Fig. 1G**). This suggests a short pulse-like or transient period of Wt1 expression during which Tam exposure allowed the recombination and labelling of future visSMCs and vSMCs cells in the midgut region. However, the labelled visSMC in the stomach and colon additionally indicate contribution along fore- and hindgut regions not limited to initiation at E7.5-E8.5.

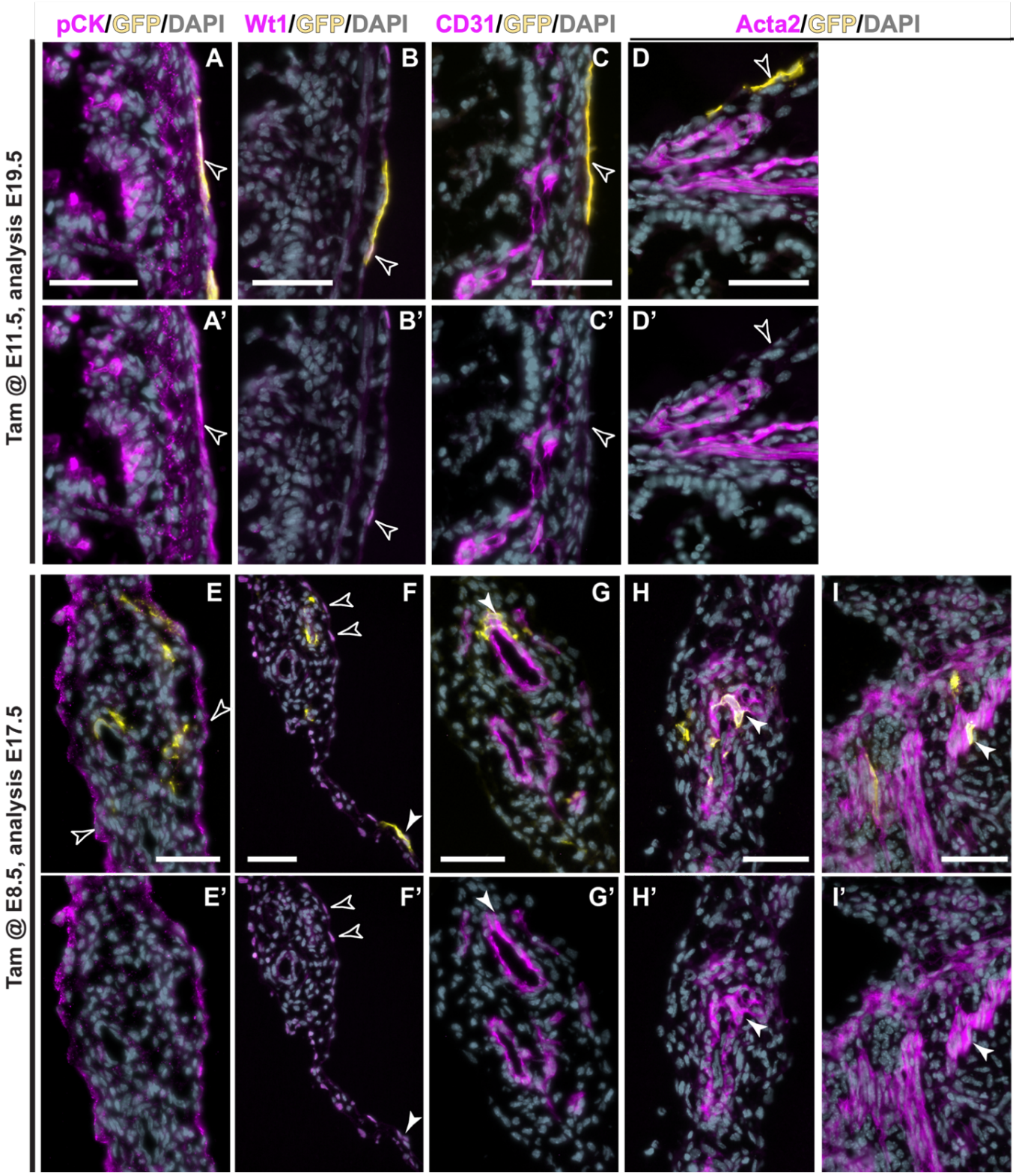

Figure 2: Immunofluorescence analysis of embryonic Wt1-lineage cells in intestine and mesentery. Frozen sections of intestine and mesentery of embryos after tamoxifen (Tam) dosing at E11.5 or E8.5, and dissection at E19.5 or E17.5, respectively) were analysed by immunofluorescence for co-expression of GFP with cytokeratin (A, A', E, E'), Wt1 (B, B', F, F'), CD31 (C, C', G, G') and Acta2 (D, D' H, H', I, I'). **A, A', B, B'.** After Tam at E11.5, the mesothelial markers cytokeratin and Wt1 were detected in the mesothelium covering the intestine and co-expression with GFP was observed in the visceral mesothelium (arrowheads). **E, E', F, F'.** After Tam at E8.5, co-expression of GFP with mesothelial markers was sparse (filled arrowhead). **C, C', D, D'.** After Tam at E11.5, expression analysis for the vascular markers CD31 and Acta2 showed no co-expression with GFP within the mesentery. **G, G'.** After Tam at E8.5, GFP-positive cells were found in close vicinity to CD31 expressed in the mesenteric vessels (arrowhead). **H, H', I, I'.** At this stage, GFP was co-expressed with Acta2 in the mesenteric vasculature (arrowhead, H, H'), and the visceral smooth muscle (arrowhead, I, I'). Scale bars, 50 µm (all).

171

172 ***Wt1* transcript is expressed from E6.5 in mouse embryos and co-expressed with**
173 **markers for smooth muscle lineage**

174 Next, we analysed expression of *Wt1* transcripts during mouse gastrulation stages E6.5 to
175 E8.5 using a published single cell RNAseq data set [21]. We found that *Wt1* was expressed in
176 mouse embryos throughout this developmental period in 0.65% to 1.66% of total embryonic
177 cells (**Supplementary Fig. 3.1A**). Mean expression for *Wt1* was between 0.955 and 1.13
178 with cells considered expressing *Wt1* if levels were above 0 (**Supplementary Fig. 3.1B**).
179 Most of the *Wt1*-expressing cells in the E7.5 embryo were found in extraembryonic
180 ectoderm, the rostral neuroectoderm, mesenchyme, epiblast and primitive streak
181 (**Supplementary Fig. 3.1C**). In E8.5 embryos, most *Wt1*-expressing cells were in the
182 mesenchyme, surface ectoderm, pharyngeal mesoderm and cardiomyocytes
183 (**Supplementary Fig. 3.1D**). Since visSMCs and vSMCs have their origin in the lateral plate
184 mesoderm (LPM) but the dataset annotation lacked a clear indication which of the
185 mesoderm tissues were LPM, we characterised in a candidate approach somatic, paraxial,
186 nascent, mixed and intermediate mesoderm together with primitive streak, notochord,
187 epiblast and mesenchyme for classical LPM and other mesodermal markers, confirming that
188 'mesenchyme' was representing the LPM population (**Supplementary Fig. 3.1E, F**).

189 Next, we selected *Wt1*-expressing cells from the epiblast, primitive streak, and mesodermal
190 tissues at stages that mapped to gastrulation (E6.5-E8.5; **Fig. 3A**). We observed a shift from
191 *Wt1*-expression mainly in the epiblast and primitive streak (E6.5 to E7.25) to expression
192 predominantly in the 'mesenchyme'/LPM from E7.5 onwards (**Fig. 3A**). When we probed for
193 *Wt1* and *Bra* co-expression (*Wt1*+/*Bra*+) in this cell population, we found that between E6.5
194 and E7.5, these cells were mostly found in the primitive streak, epiblast and nascent
195 mesoderm. By contrast, from E7.5 onwards, there was a shift of *Wt1*+/*Bra*+ co-expressing
196 cells to the intermediate mesoderm, LPM, somitic mesoderm and neuro-mesodermal
197 progenitor pool (NMP; **Fig. 3B**). Mean expression levels in *Wt1*+ *Bra*+ co-expressing cells
198 were higher for *Bra* (range 1.2 to 1.8) compared to *Wt1* (0.95-1.05; **Fig. 3C**). These data
199 show that *Wt1* expression shifted from the emerging mesoderm to the LPM as gastrulation
200 progressed. Furthermore, *Wt1* was co-expressed with gastrulation marker *Bra* in a few cells
201 of key tissues of the forming mesoderm.

202 We then further interrogated the *Wt1*-expressing population (epiblast, primitive streak,
203 mesodermal) for co-expression of LPM and smooth muscle markers, including *Hand1*,
204 *Transgelin* (*Tagln*), *Acta2* and *Pdgfrb*. Our analysis found that *Wt1* and *Hand1* were co-

205 expressed already in the epiblast, primitive streak, nascent mesoderm and LPM at E7.0,
206 and from E7.5 onwards predominantly in the LPM (**Fig. 3D**). Mean expression levels of
207 *Hand1* rose over the course of development to 3.5 at E7.5, while levels of *Wt1* were steady
208 at about 1 (**Fig. 3H**). Cells co-expressing *Wt1* and *Tagln* were already present in epiblast
209 cells at E6.5, before being found in primitive streak, nascent mesoderm and at later stages
210 predominantly in the LPM (**Fig. 3E**, **Supplementary Fig. 3.2A**). Mean expression levels of
211 *Tagln* rose over the course of development to 3 at E8.5, while levels of *Wt1* increased to
212 just above 1 (**Fig. 3I**). Similar patterns were observed for cells co-expressing *Wt1* and *Acta2*
213 (**Fig. 3F, J**) or *Wt1* and *Pdgfrb* (**Fig. 3G, K**), respectively, starting only to be co-expressed
214 from E7.5 onwards, but again predominantly in the LPM. Mean expression levels for *Wt1*
215 and *Acta2* in these cells followed a similar trajectory as for *Wt1* and *Tagln*, where *Acta2*
216 reached a level of 4, while *Wt1* rose to just above 1 (**Fig. 3J**). By contrast, the mean
217 expression levels of *Pdgfrb* and *Wt1* in co-expressing cells dropped and then increased
218 again from E7.5 to E8.5 (**Fig. 3K**). Mesodermal cells that co-expressed *Wt1*, *Tagln* and
219 *Hand1* were found at E7.0 in the primitive streak, nascent mesoderm and LPM (**Fig. 3L**).
220 Cells that co-expressed *Wt1*, *Tagln* and *Acta2*, were identified almost exclusively in the LPM
221 from E7.5 to E8.5 (**Fig. 3M**). Furthermore, the trajectories of mean expression levels of these
222 markers and cell numbers of the triple-expressing cells were similar to those observed for
223 dual co-expressing cells (**Fig. 3L, M, N, O**), indicating that in the population of *Wt1*-
224 expressing cells at stages between E7.5 to E8.5 a considerable proportion consisted of
225 *Hand1*-, *Tagln*- and *Acta2*-co-expressing cells. This is confirmed in a Venn diagram showing
226 that on average 25 mesodermal cells (23.1%) in E8.5 embryos expressing *Wt1*, co-
227 expressed *Hand1*, *Acta2*, *Tagln* and *Pdgfrb* (**Fig. 3T**), indicating their commitment to a SMC
228 fate. Of all mesodermal cells that expressed *Hand1* and/or *Acta2* and/or *Tagln* and/or *Pdgfrb*
229 and <u>not</u> *Wt1*, only 9.2% expressed all 4 genes (**Fig. 3U**). It is important to note that by
230 selecting for *Wt1*-expression in the mesodermal population of *Hand1*/*Acta2*/*Tagln*/*Pdgfrb*-
231 expressing cells, cell numbers are smaller than in the mesodermal population of
232 *Hand1*/*Acta2*/*Tagln*/*Pdgfrb*-expressing cells that did not express *Wt1*. This suggests that
233 Wt1-expression is observed in a subpopulation of this group of cells, but that these cells
234 have a clear commitment along the SMC lineage.

235 These data suggest that a consistent population of *Wt1*-expressing cells arises from the
236 epiblast, via the primitive streak to the emerging mesoderm and the LPM which co-
237 expressed *Hand1* as LPM marker, and further key markers and regulators of smooth muscle
238 fate and differentiation. Importantly, levels of *Acta2* and *Tagln* expression rose during these
239 developmental stages also in cells that did not co-express *Wt1* (**Supplementary Fig. 3.2B**).

240 We further probed the relationship of *Wt1* expression in cells undergoing differentiation
241 towards smooth muscle by assessing the co-expression of *Wt1* with myocardin-related
242 factors *MrtfA* and *MrtfB* (**Fig. 3P, Q, R, S**). Both smooth muscle regulating genes were co-
243 expressed with *Wt1* in cells of the epiblast and primitive streak, shifting from E7.5
244 predominantly towards LPM cells. Mean expression levels of *Wt1* and *MrtfA* or *Wt1* and
245 *MrtfB* were very similar at levels between 0.5 and 1 (*Wt1*/*MrtfA*) and 0.7 and just above 1
246 (*Wt1*/*MrtfB*). These results indicate that *Wt1* is co-expressed with markers and regulators of
247 smooth muscle differentiation during stages before, during and immediately after mesoderm
248 formation and specification.

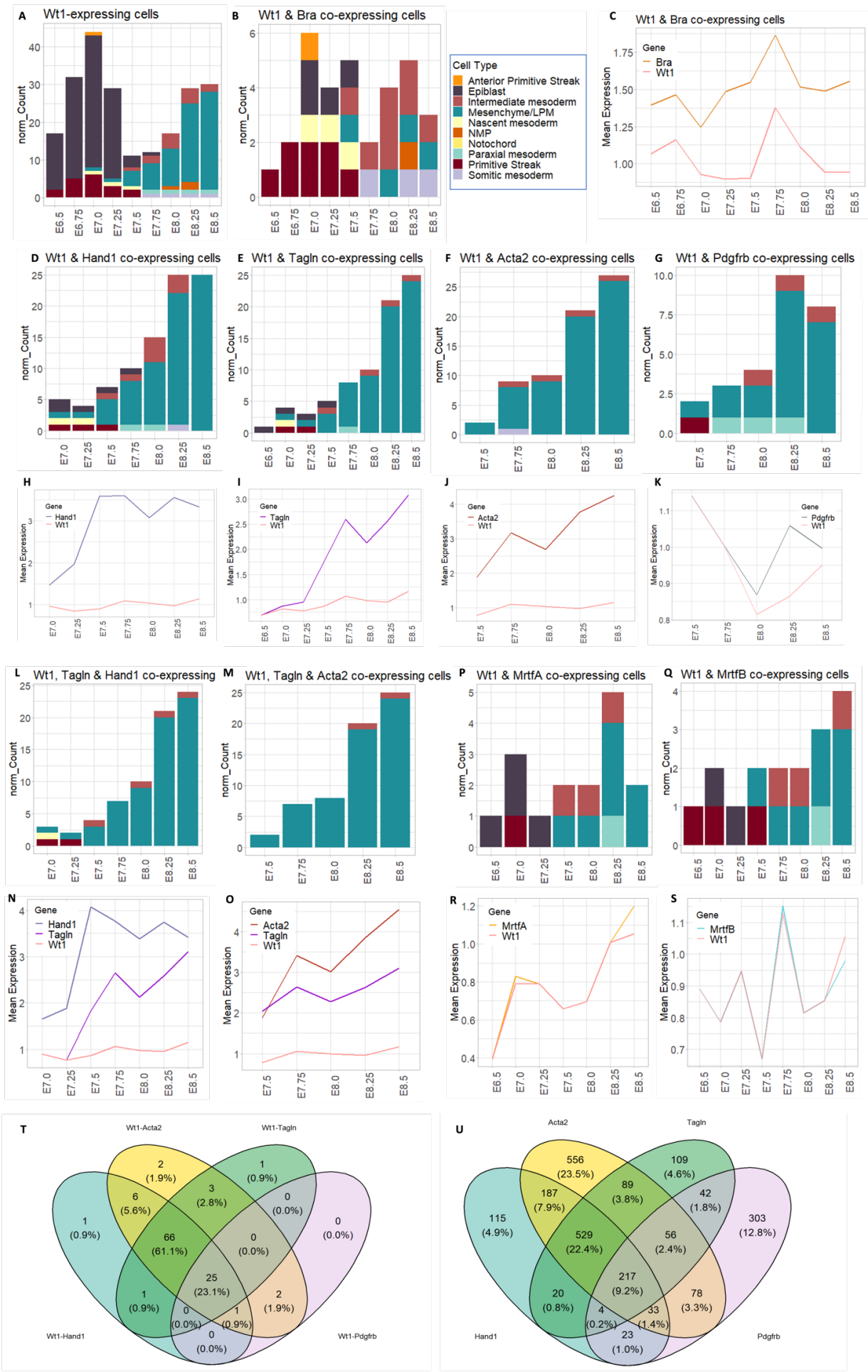
A Wt1-expressing cells
B Wt1 & Bra co-expressing cells
C Wt1 & Bra co-expressing cells
Cell Type
Anterior Primitive Streak
Epiblast
Intermediate mesoderm
Mesenchyme/LPM
Nascent mesoderm
NMP
Notochord
Paraxial mesoderm
Primitive Streak
Somitic mesoderm
Gene
Bra
Wt1
Mean Expression
norm_Count
D Wt1 & Hand1 co-expressing cells
E Wt1 & Tagln co-expressing cells
F Wt1 & Acta2 co-expressing cells
G Wt1 & Pdgfrb co-expressing cells
H
I
J
K
L Wt1, Tagln & Hand1 co-expressing
M Wt1, Tagln & Acta2 co-expressing cells
P Wt1 & MrtfA co-expressing cells
Q Wt1 & MrtfB co-expressing cells
N
O
R
S
T
Wt1-Acta2
Wt1-Tagln
Wt1-Hand1
Wt1-Pdgfrb
U
Acta2
Tagln
Hand1
Pdgfrb

Figure 3: Distribution of *Wt1*-expressing cells in the mesoderm and presumptive smooth muscle cell lineage in gastrulation stage embryos. A-C. Distribution of *Wt1*-expressing cells from E6.5 to E8.5 together with early mesoderm marker, *Bra*, in mesodermal cells. *Wt1* transcripts were originally detected in epiblast and primitive streak cells and gradually (E7.5 to E7.75) shifted into cells of mesoderm lineage, predominantly lateral plate mesoderm and its derivatives. **D-K.** Distribution of *Wt1*-expressing cells in mesodermal tissues that co-expressed LPM and early SMC markers *Hand1*, *Tagln*, *Acta2* or *Pdgfrb*. *Wt1* transcripts were identified in epiblast and primitive streak cells that co-expressed *Hand1* at E7.0 (D, H), or *Tagln* at E6.5 (E, I), but from E7.5 onwards, these cells were mainly found in the LPM. Similar dynamics were observed for *Wt1*-expressing cells that co-expressed *Acta2* (F, J) or *Pdgfrb* (G, K). A small number of cells co-expressing *Wt1* and any of the SMC markers also contributed to intermediate mesoderm cells. **L-O.** Triple co-expression of *Wt1* with *Tagln* and *Hand1* or *Wt1* with *Tagln* and *Acta2* was predominantly detected in cells of the LPM, from E7.5 onwards. **P-S.** Co-expression of *Wt1* with the myocardin-related transcription factors (Mrtf) *MrtfA* and *MrtfB* in mesodermal tissues was found in small number of cells at E6.5, where expression was found in epiblast and primitive streak cells. Co-expressing cells were later detected in the lateral plate mesoderm, intermediate mesoderm and paraxial mesoderm. **T, U.** Venn diagram of mesodermal cells that expressed *Wt1* and co-expressed *Hand1*, *Acta2*, *Tagln* and/or *Pdgfrb* (T). Note that these numbers encompass the cells of the four E8.5 embryos that had been sequenced in (Pijuan-Sala et al. 2019). (U) shows the Venn diagram for mesodermal cells expressing *Hand1*, *Acta2*, *Tagln* and/or *Pdgfrb* when *Wt1*-expressing cells are not considered.

Our *in vivo* lineage tracing results indicated that Wt1 expression at between around E7.5 to E8.5 primed a group of emerging mesoderm cells towards SM fate, but not mesothelial fate. To determine whether mesothelial markers were co-expressed with *Wt1* during gastrulation stages, we interrogated the scRNAseq data for co-expression of *Wt1* with mesothelial progenitor marker *Hand2* (see also paralogous gene *Hand1* in **Fig. 3**), mesothelial-specific markers *Podoplanin* (*Pdpn*), *Epicardin* (*Tcf21*), *Uroplakin 3b* (*Upk3b)* and *Tbx18*. Our results showed that cells co-expressing *Wt1* and *Hand2* were mostly found in the LPM from E7.0 onwards, and expression levels of *Hand2* reached 1.4 (**Supplementary Fig. 3.2G, K**). Onset of mesothelial gene expression in *Wt1*-expressing cells varied between E6.5 (*Pdpn*, **Supplementary Fig. 3.2D, H, L**) and E8.25 (*Tbx18*, **Supplementary Fig. 3.2D, O, P**). *Tcf21* and *Upk3b* started to be co-expressed in *Wt1*-expressing cells at E7.0 and E7.5, respectively (**Supplementary Fig. 3.2 D, I, J, M, N**). In all cases, the majority of co-expressing cells were found in the LPM. However, there was little overlap in the co-expression between these mesothelial markers with *Wt1* in the E8.5 mouse embryo (**Supplementary Fig. 3.2Q, R**). This suggests that mesothelial cell identity or fate was not robustly established yet in *Wt1*-expressing mesodermal cells in the LPM in the E8.5 embryo.

Wt1 protein is expressed in the primitive streak and emerging mesoderm in E7.5 and E8.5 mouse embryos

Next, we determined Wt1 protein expression in E7.5 and E8.5 mouse embryos using confocal immunofluorescence microscopy of whole mount embryos, and found that Wt1 was expressed in the tail bud of E8.5 embryos, as well as extra-embryonic tissues including the yolk sac and allantois (**Fig. 4 A-C**). Co-immunostaining with Bra and confocal imaging

clearly identified Wt1-expressing cells in the Bra-domains of primitive streak and IM/LPM region (**Fig. 4A, C, D-G**; compare **Supplementary Fig. 4** based on the EMAP eMouse Atlas project [22]). Co-expression analysis of individual focal planes revealed that in the most posterior region around the primitive streak, Wt1 expression was found in some Bra-positive cells emerging from the node (**Fig. 4E**), the mesenchyme including neuromesodermal progenitor cells and LPM/IM, the neural plate, primitive blood cells and allantois (**Fig. 4D-G;** and insets). Quantification of co-expression of Wt1 and Bra in the insets of **Fig. 4E, F** revealed that cells with strong Wt1 expression, also were positive for strong Bra expression (**Fig. 4H**), confirming that Wt1 was co-expressed in Bra-positive cells emerging from the mesoderm. Of note, the scRNAseq dataset suggested that very few cells contained transcripts of both *Wt1* and *Bra*, while protein for both genes seemed to be detectable in more cells.

At E7.5, the co-expression domain between Wt1 and Bra was more restricted, with Wt1 mostly expressed in the epiblast, where it was co-expressed with Bra, and in the primitive streak (**Supplementary Fig. 5B**).

Further confocal image analysis of triple whole mount immunofluorescence for Wt1, Bra and Tagln in E8.5 mouse tailbuds demonstrated protein co-expression of Wt1 with Tagln in the mesoderm/paraxial mesoderm and LPM (**Fig. 4I-N** and **Supplementary Fig. 5A**). These data support the observation that co-expression of Wt1 and Tagln in the emerging LPM define the smooth muscle population.

Taken together, these data show that Wt1 is dynamically expressed in the gastrulating embryo: in cells of the primitive streak and emerging mesoderm including the neuromesodermal progenitor cells and LPM, where it is co-expressed with SMC markers.

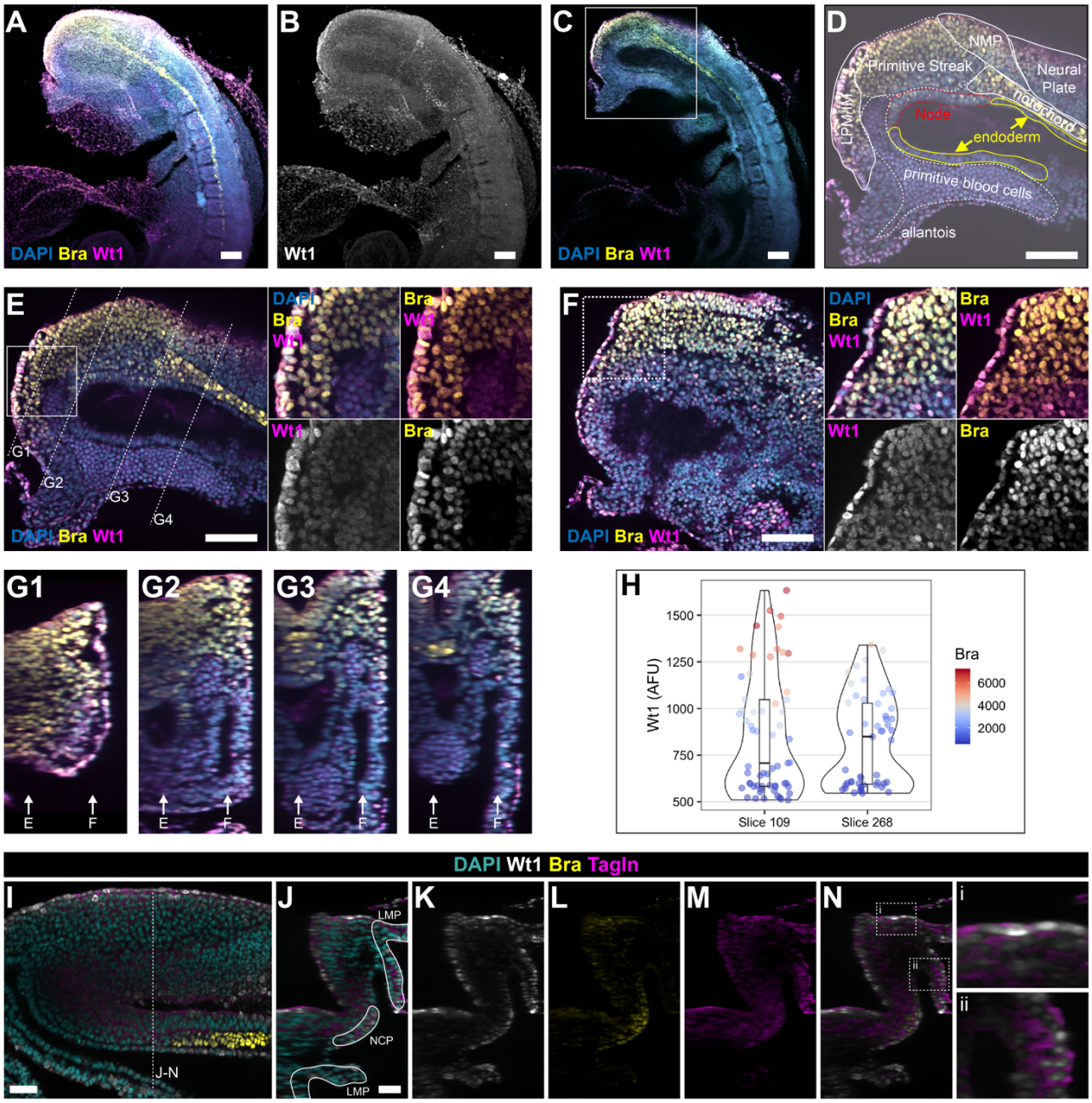

Figure 4: Wt1 is expressed in the primitive streak, emerging mesoderm, NMP and LPM in E8.5 mouse embryos. A-D. Whole mount staining for Wt1 and Bra in the E8.5 mouse tail bud. A and B are MIP images generated from 150 z-sections, while C and D are focal images at sagittal level. Wt1 was expressed in the tail bud, in the allantois and yolk sac, as well as primitive streak, NMP, LPM/IM, where there was co-expression with Bra. In D (based on E), the different tissue domains are outlined. **E-G.** Images at two focal planes through the tail bud including node, primitive streak, notochord, NMP, LPM/IM and neural plate, in sagittal (slice 109, E), and near-sagittal (slice 268, F) position. Boxes in E and F indicate position of higher magnified inserts. Lines in E indicate position of focal views in G1-4. Arrows in G-14 indicate position of focal planes for E and F. **H.** Quantification of co-expression levels of both Wt1 and Bra at the two focal slices indicated shown in E and F and indicated in G1-4. AFU: arbitrary fluorescence units. **I.** Whole mount staining for Wt1, Bra and Tagln in the E8.5 mouse tail bud. Image of oblique focal plane; stipled line indicates focal plane for images J-N. **J.** LPM and notochordal plate (NCP) are outlined in transverse focal plane image. **K-M**. Expression of Wt1 (K), Bra (L) and Tagln (M). Wt1 and Tagln were co-expressed in the surface cells covering the paraxial mesoderm and in the LPM. Scale bars, 100 µm (A-E), 50 µm (I-N).

297

298

299 **Cells arising from *Wt1*-lineage tracing after Tam dosing at E7.5 or E8.5 localise to**
300 **three main tissues at E9.5: pro-epicardium, urogenital ridge and neural tube.**

301 To obtain a better temporal resolution of the cells that had expressed Wt1 at gastrulation
302 stages for lineage tracing of SMCs, we decided to repeat the E7.5 and E8.5 Tam dosing
303 and observe the range and localisation of GFP-positive cells at the earlier E9.5 time-point
304 (**Fig. 5**).

305 When we administered Tam at E8.5 and analysed at E9.5, abundant GFP-positive cells
306 where localised to the pro-epicardium at the caudal side of the forming heart
307 (**Supplementary Fig. 6A-D**), and to the urogenital ridge (**Fig 5**, **Supplementary Fig. 6A,**
308 **B, C'**). We observed GFP-positive cells consistently towards the ventral midline, including
309 the mesentery, in sections, and by using light sheet microscopy of the trunk region of the
310 E9.5 embryo (**Fig. 5**, **Supplementary Fig. 7**, **Supplementary Movie, Supplementary**
311 **Table 2**). By contrast, Tam dosing at E7.5 resulted in less GFP-positive cells, which were
312 mostly found in the pro-epicardium (**Supplementary Fig. 6E-G**). In three litters analysed,
313 we found that all 15 embryos had between 2 and 20 GFP-positive cells in the pro-
314 epicardium, while GFP-positive cells (range 1-12) in the posterior trunk region were
315 observed only in 9 out of 15 embryos (**Supplementary Table 3**, **Supplementary Fig. 8**).
316 Importantly, we also detected GFP-positive cells in the neural tube of embryos after Tam at
317 E7.5 (**Supplementary Fig. 6H-K**) and E8.5 (not shown), in line with our observations in
318 **Figs. 3** and **4** that Wt1 was also expressed in the emerging neuroectoderm.

319 Together, these results demonstrate that the *Wt1*$^{CreERT2/+}$ lineage tracing system detected
320 cells that expressed Wt1 at around E7.5 and E8.5 within a similar spectrum of cell progeny,
321 but GFP-positive cell numbers where smaller when Tam was given at E7.5. This was in
322 agreement with the scRNAseq data analysis (**Fig. 3**) and distribution of Wt1-expressing cells
323 by whole mount immunofluorescence (**Fig. 4**). Moreover, we could identify GFP-positive
324 cells that appeared in the region of the mesentery, as potential precursors for visceral and
325 vascular smooth muscle of the developing intestinal tract.

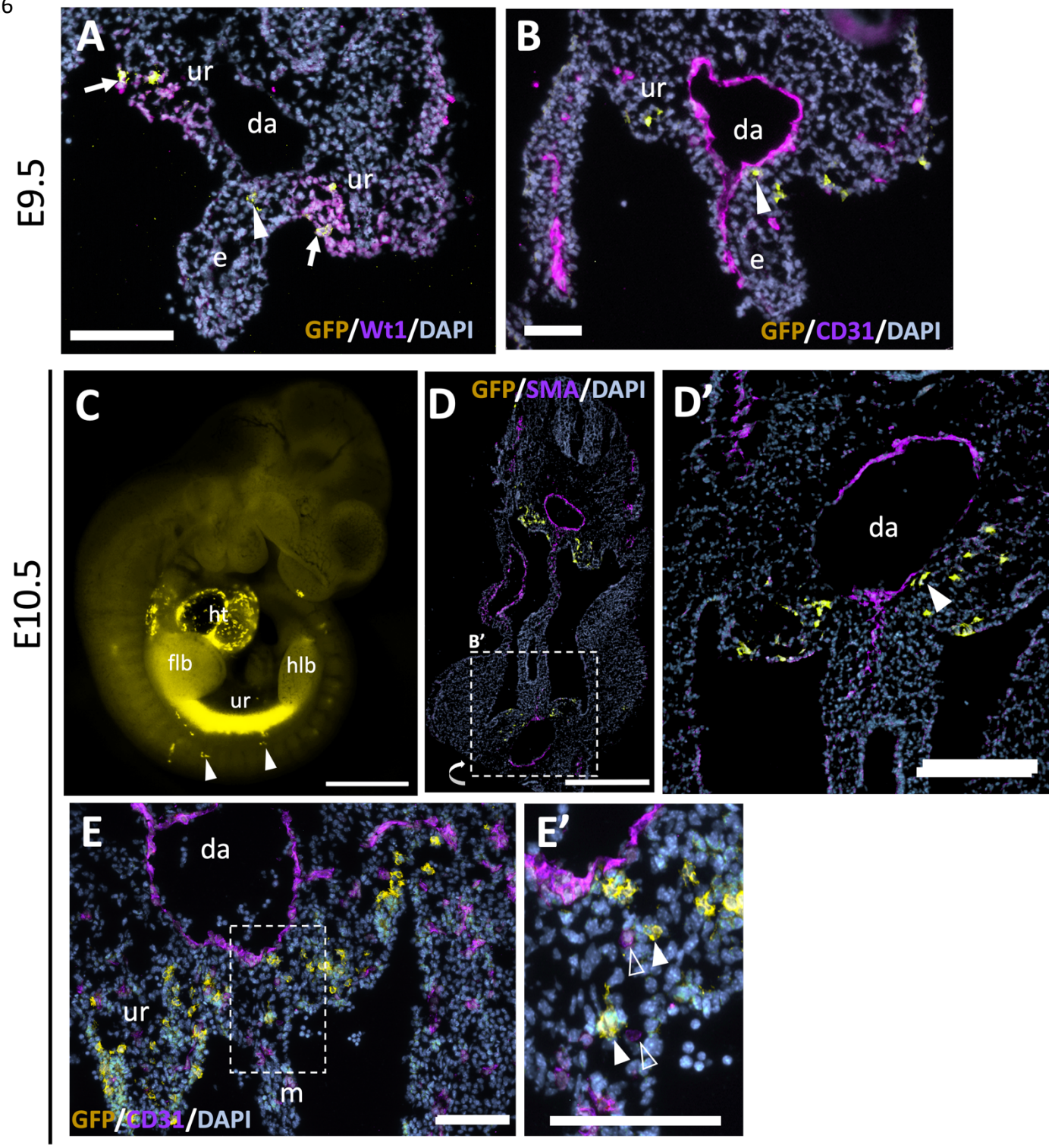

Figure 5: Localisation of Wt1-lineage cells in the urogenital ridge and close to the mesentery near endothelial cells. A, B. Immunofluorescence staining for GFP and Wt1 (D) and GFP and CD31 (E) on sections through E9.5 embryos after Tam dosing at E8.5. GFP-positive cells were detected in the region between dorsal aorta (da) and mesentery, besides presence in the urogenital ridge (ur). **C.** Representative overview image of embryo at E10.5 after Tam dosing at E8.5. GFP-positive cells were most prominent in the heart (ht), and urogenital ridge (ur). Arrowheads point to individual cells dorsally away from the main ur expression domain. **D, D'.** Immunofluorescence staining for GFP and SMA on sections through the region just below the forelimb bud. GFP-positive cells were localized in the urogenital ridge and close to the dorsal aorta (da)(arrowheads). **E, E'.** Immunofluorescence staining for GFP and CD31 on section through similar embryonic level as in D. GFP-positive cells were also found ventral to the dorsal aorta and dorsal to the mesentery, closely associated with cells of the endothelial plexus (filled arrowhead: GFP+, open arrowhead: CD31+). da, dorsal aorta, e, endoderm, flb, forelimb bud, hlb, hindlimb bud, ur, urogenital ridge. Scale bars, 1000 µm (A), 500 µm (B), 250 µm (B'), 100 µm (C, C', D), 50 µm (E).

327 **Cells of the *Wt1*-lineage contribute to the development of the vascular and visceral**
328 **smooth muscle between E10.5 and E15.5**

329 To elucidate the developmental path and fate of the vSMCs and visSMCs using the
330 emergence of the GFP-positive cells, we analysed embryos at E10.5 after Tam dosing at
331 E8.5. At this stage, GFP-positive cells were predominantly seen in the region of the
332 urogenital ridge and the heart (**Fig. 5C**). In tissue sections, GFP-positive cells localised in
333 the region between the dorsal aorta and the ventral mesentery, and within the urogenital
334 ridge (**Fig. 5D, D'**). Some of the cells within the region between dorsal aorta and ventral
335 mesentery appeared to be situated close to endothelial cells (**Fig. 5E, E'**).

336 In embryos at E12.5, we found GFP-positive cells in a spotty appearance within the
337 mesentery of the developing small intestinal segment of the intestinal tract (**Fig. 6B, B'**).
338 Immunofluorescence analysis on sections through this region revealed that GFP-positive
339 cells were localised within the mesentery and in the developing intestinal wall near the
340 forming vascular plexus (**Fig. 6C, D**). GFP-expressing cells were distinct from endothelial
341 cells but closely associated (**Fig. 6D**). Furthermore, our analysis showed that some of the
342 GFP-labelled cells within the mesentery and the intestinal wall co-expressed Pdgfrb,
343 suggesting that they had started the smooth muscle differentiation programme (**Fig. 6E, F-**
344 **F''**). Occasionally, we found a few GFP-positive cells in the mesothelial covering of the
345 mesentery (**Fig. 6E, F**). Together, these results indicate that *Wt1*-lineage traced cells
346 labelled at around E8.5, appeared in the vicinity of the developing vasculature and co-
347 expressed Pdgfra, a key marker of vascular smooth muscle progenitor cells during stages
348 of intestinal patterning and angiogenesis. When endpoint analysis was performed at E15.5,
349 we detected GFP-positive cells within the visceral smooth muscle and surrounding
350 mesenteric vessels (**Fig. 6G-H**), similar to findings from the endpoint analysis at around
351 E18.5 (**Fig. 1I**).

352

353

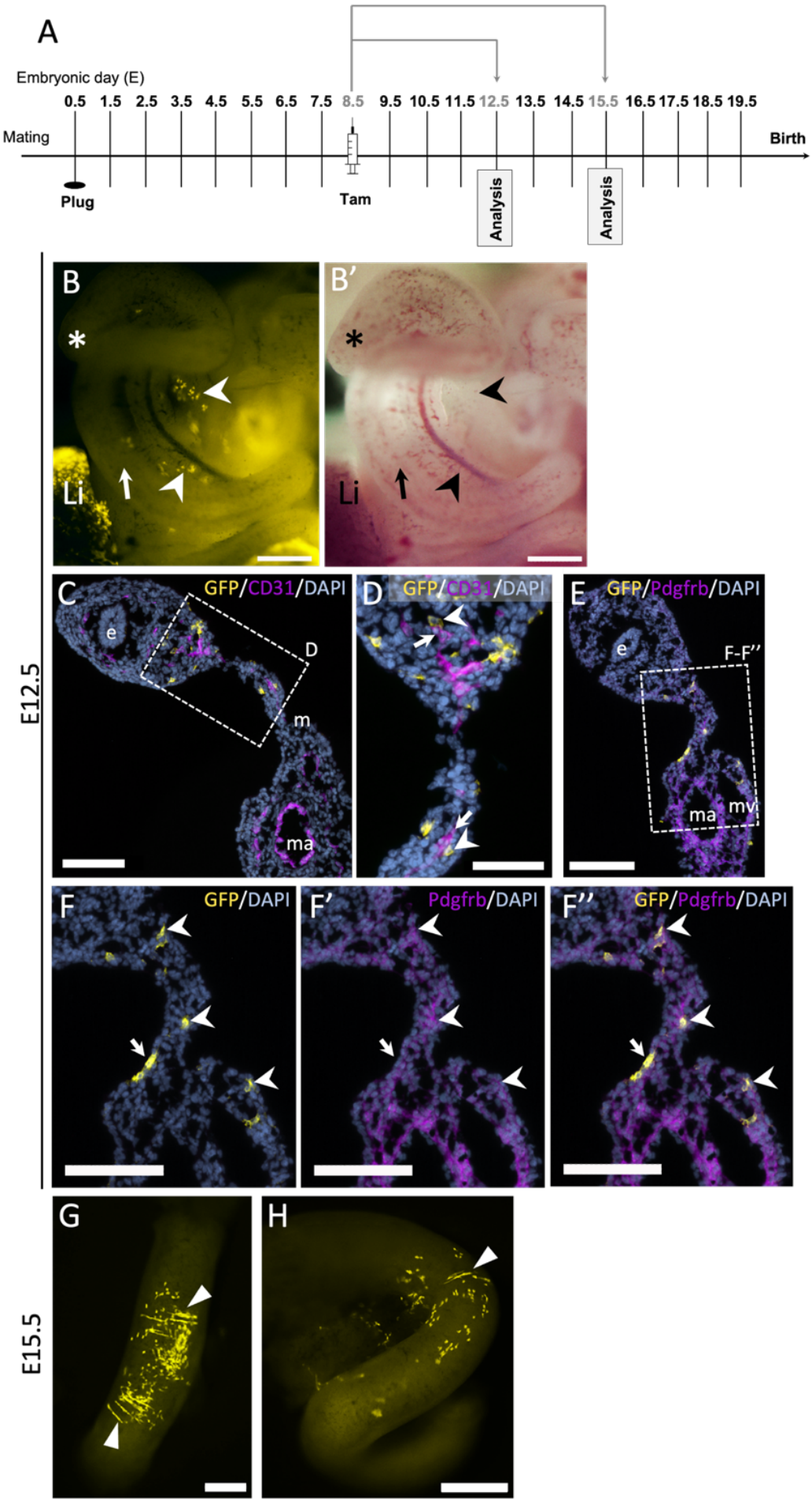
A
Embryonic day (E)
0.5 1.5 2.5 3.5 4.5 5.5 6.5 7.5 8.5 9.5 10.5 11.5 12.5 13.5 14.5 15.5 16.5 17.5 18.5 19.5
Mating
Birth
Plug
Tam
Analysis
Analysis
B
B'
Li
Li
E12.5
C
GFP/CD31/DAPI
e
D
m
ma
D
GFP/CD31/DAPI
E
GFP/Pdgfrb/DAPI
e
F-F''
ma
mv
F
GFP/DAPI
F'
Pdgfrb/DAPI
F''
GFP/Pdgfrb/DAPI
E15.5
G
H

Figure 6. Contribution of *Wt1*-lineage cells to the mesentery near developing vasculature and to the intestinal wall. A. Schematic of the study design: analysis of embryos at E12.5 or E15.5 after time mating of *Wt1*$^{CreERT2/+}$;*Rosa26*$^{mTmG/mTmG}$ males with CD1 females and Tam dosing at E8.5. **B, B'.** View of the intestinal loop and mesentery. GFP-positive cells (chevrons) were found within the mesentery of the developing intestinal tract (arrow; star depicts caecum). Note the abundant GFP fluorescence in the liver (Li). **C-D.** Immunofluorescence of CD31 and GFP on sections through this region showed GFP-positive cells within the mesentery and in the intestinal wall, near the developing microvascular plexus (C). Higher magnification (D) reveals that GFP-positive cells (chevrons) are often arranged close to neighbouring endothelial cells (arrows) of the vascular plexus in the intestinal wall and mesentery. **E-F''.** Immunofluorescence for Pdgfrb and GFP on neighbouring sections showed that GFP-positive cells within the intestinal wall mesenchyme and mesentery co-expressed Pdgfrb (chevrons), while a few mesothelial GFP-positive cells were Pdgfrb-negative (F-F'', arrow). **G, H.** Representative images from two different embryos at E15.5 after tamoxifen dosing at E8.5. GFP-positive cells (arrowheads) were found within a segment of the small intestine in a circular arrangement. da, dorsal aorta, e, endoderm, m, mesentery, ma, mesenteric artery, mv, mesenteric vein. Scale bars, 500 µm (G, H), 300 µm (B, B'), 100 µm (C, E, F-F''), 50 µm (D).

355

356

357 **Discussion**

358 In this study, we have for the first time determined the temporal and spatial relationship
359 between the emerging intestinal vascular and visceral smooth muscle cells and the
360 expression of the transcriptional regulator Wt1 during gastrulation and post-gastrulation
361 stages of mouse embryonic development. Our analysis revealed that Wt1 is expressed in a
362 progenitor cell pool in the emerging mesoderm of the gastrulating embryo. Some of these
363 cells differentiate into smooth muscle cells in the intestine and mesentery. Our data indicate
364 that this process is temporally independent of the formation of the mesothelium covering
365 these tissues, which also expresses Wt1. Thus, our data shed new light onto smooth muscle
366 development independent from mesothelium development, and the temporo-spatial
367 involvement of Wt1 in this process (**Supplementary Fig. 9**).

368

369 Here, using Tam-dependent, inducible genetic lineage tracing, we analysed the embryonic
370 contribution of Wt1-expressing cells to visSMCs and vSMCs of the intestine. In previous
371 studies, we had shown that Wt1-expessing cells give rise to vSMCs in the mesentery and
372 intestine using a non-inducible Wt1-based lineage tracing system [13]. Similarly, by using the
373 same or an alternative Wt1-driven genetic reporter system, it had been demonstrated that
374 Wt1-expressing progenitor cells give rise to visSMCs and vSMCs not only in the intestine
375 but also in the lungs [15,18,23], however, the temporal involvement and spatial significance of
376 Wt1 expression during smooth muscle specification and differentiation had not been
377 determined.

378 In a follow-on study, we determined that Wt1-expressing cells in postnatal stages fail to give
379 rise to intestinal visSMCs and vSMCs, by making use of the same Tam-dependent temporal
380 activation process for lineage analysis as utilised here (Wilm et al., 2021). We concluded
381 that the source of intestinal and mesenteric SMCs had to be cells expressing Wt1 during
382 embryonic development; however, it was not clear whether these cells arise from the
383 overlying mesothelium which also expresses Wt1 during embryonic development, as had
384 been our previous hypothesis [13].

385 To address this question, we administered Tam between E7.5 and E13.5 using the
386 *Wt1*$^{CreERT2/+}$ driver in combination with either the *Rosa26*^{LacZ} or *Rosa26*^{mTmG} reporter
387 systems, and analysed the presence of LacZ- and GFP-labelled cells in foetuses just before
388 birth (E17.5, E18.5 or E19.5). Our analysis showed that Tam dosing at E7.5 or E8.5 resulted
389 in labelling of vSMC and visSMCs which had originated from Wt1-expressing cells. When

390 Tam was given at E9.5 or later stages, the labelled cells were confined to the mesothelial
391 covering of the mesentery and intestine. This finding demonstrates a clearly defined
392 separate mechanism of the emergence of the mesothelial lineage, from the vascular/visceral
393 smooth muscle lineage, indicating a role for Wt1 in distinct mechanisms.

394 Other studies have previously used the Tam-inducible *Wt1*$^{CreERT2/+}$ driver in combination with
395 reporter systems to elucidate the lineage and origin of smooth muscle cells in the lungs.
396 Contribution to airway smooth muscle, vascular smooth muscle and parenchyma was
397 observed in late-stage mouse foetuses when Tam had been given between E9.5 and E11.5
398 [24,25]. Time lapse experiments of *ex vivo* cultured lungs from lineage-traced E12.5 embryos
399 after Tam at E10.5 revealed a direct contribution of mesothelial cells towards the deeper
400 lung parenchyma [24]. These results suggest that the smooth muscle of the airways and lung
401 vasculature may have a contribution via the mesothelium at later developmental stages, in
402 a different mechanism to the one described here for the intestinal tract.

403 In the heart, Wt1-based lineage tracing had demonstrated contribution of epicardial cells to
404 coronary vessel formation [13,17,26,27]. Based on *in situ* hybridisation and immunofluorescence
405 on sections of E8.5 embryos, Wt1 was not expressed in the developing heart at this stage.
406 By contrast, non-inducible *Wt1*^{CreEGFP};*Rosa26*^{mTmG} embryos at E8.5 had a number of GFP-
407 expressing cells in the forming heart, indicating an early contribution of Wt1-expressing cells
408 [26]. However, Wt1 is also expressed in non-epicardial cells in the heart, including
409 myocardium, which makes interpretation of lineage experiments more challenging [26]. In
410 addition, our own post-natal lineage tracing experiments using the Tam-inducible
411 *Wt1*$^{CreERT2/+}$ driver had shown that after birth Wt1-expessing cells contribute to coronary
412 SMCs [14], suggesting a different mechanism of coronary angiogenesis and maintenance of
413 coronary vasculature than in the intestinal tract and mesentery.

414

415 The Tam-inducible lineage tracing system is dependent on the Tam-driven recombination
416 activity which then irreversibly switches on the reporter gene expression. Several studies
417 have analysed the temporal delay between Tam administration and reporter expression,
418 indicating that depending on route of administration (oral gavage or IP injection), a temporal
419 delay of between 12-18 hours could be observed in other genetic systems [28,29]. This
420 temporal delay needs to be factored in when interpreting the results of the current study,
421 suggesting that about 0.5 embryonic days may have to be added to the stages indicated for
422 the recombination initiation.

423

424 One of the surprising findings of this study emerged from our analysis of scRNAseq data [21]
425 showing that from E6.5 onwards, *Wt1* is expressed in the epiblast, primitive streak and
426 emerging mesoderm, and in the LPM where it is co-expressed with key markers of SMC
427 development. We could confirm co-expression of Wt1 protein with Bra in the primitive
428 streak/emerging mesoderm, and with the key SM marker Tagln in the LPM.

429 Analysis of Wt1 expression in early stage mouse embryos had been previously performed
430 by in situ hybridisation showing *Wt1* transcripts in the intermediate mesoderm/LPM in E9.0
431 mouse embryos [8]. Because further insights into Wt1 expression or function at gastrulation
432 stages have not been published yet, our results are the first to shed light onto Wt1
433 gastrulation-stage expression or engagement. We have identified Wt1 expression in epiblast
434 and primitive streak cells in embryos up to about E7.25, and then a shift to specifically
435 identified mesodermal cells in E8.5 embryos where they are predominantly present in the
436 LPM. Our results reveal critical expression of Wt1 in a progenitor pool of SMCs, which may
437 represent the precursors of the visSMCs and vSMCs labelled in the lineage tracing studies.
438 With these results we have demonstrated that Wt1-expressing cells unexpectedly emerge
439 already in gastrulation stage embryos as the precursors for intestinal visSMC and vSMC,
440 providing a direct link for Wt1 with SMC fate.

441

442 The peritoneal mesothelium emerges due to separation of the LPM into somatic and
443 splanchnic mesoderm, which surround the peritoneal cavity; the splanchnic mesoderm
444 forms the mesodermal component of the intestinal tract [30]. Detailed analysis of the
445 emergence of the mesothelium has been provided in chick and quail embryo models [31,32],
446 demonstrating that the bilateral splanchnopleure consisting of splanchnic mesoderm and
447 endoderm, turns into a trilaminar tissue with a mesenchymal layer emerging between an
448 outer mesodermal epithelium and the endoderm. While in the chick embryo, the outer
449 epithelium is situated on a basal lamina already at HH13 (~19 somites, 48 hours),
450 cytokeratin expression as indicator for epithelium, starts only at HH19 (~40 somites, 71
451 hours; roughly corresponding to mouse embryos at Theiler stage 17 or E10.5), and Wt1 is
452 not expressed at this stage yet [32]. The outer epithelium is defined as mesothelium only from
453 HH29 (6 days) onwards (chick and quail), when it has organised into a simple squamous
454 epithelium [31,32].

455 In zebrafish, *hand2* expression has been presented as a marker for mesothelial progenitor
456 cells emerging from the lateral most region of the LPM at tailbud stage (i.e. at late
457 gastrulation stages) [33]. Co-expression with Tagln in the LPM-emerging cells, and a more

limited expression of *wt1a/b*, that was restricted to the cells of the anterior visceral peritoneum, and absent posteriorly and in the parietal mesothelium, suggested that *hand2* was a more encompassing marker for arising mesothelium. Furthermore, *hand2* mutant zebrafish had disorganised LPM-derived cells, in particular a lack of parietal mesothelium, indicating an upstream regulatory role of *hand2* in mesothelium formation [33].

In the mouse embryo, the peritoneal mesothelium has been shown to arise between E10.5 and E11.5 since at E11.5, a continuous layer of cells expressing cytokeratin and Wt1 is present [13]. Further information on mesothelial precursor populations and lineage in mouse embryonic development is limited: non-inducible Hand2 or Hand1-based lineage tracing showed labelling of mesothelium over the liver in E14.5 or E15.5 mouse embryos but no temporal analysis [33]. Non-inducible Hand1-lineage has also been shown to label the visceral smooth muscle in mouse embryos at E14.5 [34]. Therefore, it is not clear whether in the mouse, Hand1 or Hand2 can be considered markers of the mesothelial precursor population.

Visceral smooth muscle arises from around E13 in the mouse embryo based on Acta2 immunofluorescence [13,35], while the vascular smooth muscle in the intestine and mesentery can be detected from E12.5 during angiogenic remodelling, with mature vessels covered by mural cells, detectable from E15.5 onwards [13,36]. A complex signalling network including the Myocardin/serum response factor (SRF) interaction controls SMC differentiation by regulating expression of cytoskeletal SM proteins including Acta2, Transgelin and smooth muscle myosin heavy chain. Furthermore, Pdgfrb signalling regulates vSMC proliferation, migration and differentiation [1]. In this study, we have shown that some of the key regulators and markers of SMC fate and differentiation are co-expressed with Wt1 already from E7.5 onwards in the LPM. In addition, at E12.5, Wt1-lineage traced cells in the developing intestinal /mesenteric vascular network co-expressed Pdgfrb after activation of the reporter at around E8.5. These results strongly suggest a role for Wt1 in smooth muscle development, originating in cells of the emerging mesoderm. Furthermore, our analysis of Wt1-lineage tracing at earlier stages (E9.5, E10.5) of development, suggest that the Wt1-lineage traced cells originating at E8.5, may migrate into the mesentery and towards the developing vascular network.

Taken together, our data clearly demonstrate that the visSMCs and vSMCs that arose from Wt1-expressing cells at around E7.5 or E8.5, are independent in their specification and differentiation from the mesothelial cells of the peritoneum. These can only be tagged after

492 initiation of Wt1-controlled recombination from around E9.5 onwards. These results indicate
493 an early emergence of visSMC and vSMC lineage in the gastrulating embryo, and an
494 uncoupling from the mesothelial lineage. The role of Wt1 in both processes remains to be
495 elucidated.

496

497 **Mice:**

498 The following compound mutants were used in this study and bred in-house: *Wt1*$^{CreERT2/+}$;
499 *Rosa26*$^{LacZ/LacZ}$ (*Wt1*$^{tm2(cre/ERT2)Wtp}$; *Gt(ROSA)26Sor/J*)[17,37], *Wt1*$^{CreERT2/+}$; *Rosa26*$^{mTmG/+}$
500 (*Wt1*$^{tm2(cre/ERT2)Wtp}$; *Gt(ROSA)26Sor*$^{tm4(ACTB-tdTomato,-EGFP)Luo}$*/J*)[38]. CD1 female mice (at least 10
501 weeks old, Charles River, Harlow, UK) were time-mated with *Wt1*$^{CreERT2/+}$;*Rosa26*$^{LacZ/LacZ}$ or
502 *Wt1*$^{CreERT2/+}$;*Rosa26*$^{mTmG/+}$ males, and when a vaginal plug was detected, noon of the day
503 was considered as embryonic day 0.5 (E0.5). CD1 female mice time-mated by Charles River
504 were ordered in. Mice were housed in individually ventilated cages under a 12-hour
505 light/dark cycle, with *ad libitum* access to standard food and water. All animal experiments
506 were performed under a Home Office licence granted under the UK Animals (Scientific
507 Procedures) Act 1986 and were approved by the University of Liverpool AWERB committee.
508 Experiments are reported in line with the ARRIVE guidelines.

509

510 **Tamoxifen dosing**

511 For Wt1 lineage tracing in embryos, pregnant CD1 mice after mating with *Wt1*$^{CreERT2/+}$;
512 *Rosa26*$^{LacZ/LacZ}$ or *Wt1*$^{CreERT2/+}$; *Rosa26*$^{mTmG/+}$ male mice were dosed with 100 µg/g body
513 weight of Tam (T5648, SigmaAldrich; 40 mg/ml, in corn oil (C8267, SigmaAldrich)) via oral
514 gavage once on various days and analysed between E9.5 and E19.5. Pregnant dams were
515 monitored for their well-being including daily weight checks.

516

517 **XGal staining**

518 Dissected embryos or tissues were fixed in 2% paraformaldehyde (PFA)/0.25%
519 glutaraldehyde in phosphate buffered saline (PBS) for between 1 and 1.5 hours, whole-
520 mount XGal staining performed overnight according to standard protocols, followed by
521 overnight post-fixation in 4% PFA (PBS) at 4°C.

522

523 **Immunofluorescence**

524 The following primary antibodies were used: anti-Wt1 rabbit polyclonal (1:200 to 1:500, clone
525 C-19, sc-192, Santa Cruz), anti-Wt1 mouse monoclonal (1:50, clone 6F-H2, M3561, Dako),
526 anti-SMA mouse monoclonal (1:100 to 1:200, clone 1A4, A2547, Sigma), anti-Pecam/CD31
527 rat monoclonal (1:50, 550274, Pharmingen), anti-Brachyury goat polyclonal (1:200, PA5-
528 46984, Invitrogen/ThermoScientific), anti-Tagln/Sm22 mouse monoclonal (1:100, 60213-1-

529 Ig, Proteintech) anti-GFP rabbit or goat polyclonal (1:5000, ab6556 or ab6673, Abcam). The
530 anti-SMA and anti-Tagln/Sm22 antibodies were directly labelled using Zenon direct labelling
531 kit (Invitrogen/ThermoScientific) according to manufacturer's instructions. Secondary
532 antibodies were Alexa fluorophore-coupled (Invitrogen/ThermoScientific) and were used at
533 a dilution of 1:1000. DAPI (D9542, SigmaAldrich) was used at 1:250-1000 for nuclear
534 counterstaining.

535 *Frozen sections:* Tissues were fixed in 4% PFA for between 30 to 90 mins, protected in 30%
536 sucrose overnight, placed in Cryomatrix (Thermo Scientific) and snap frozen. Frozen
537 sections were generated at 8-10 µm on a Thermo Scientific HM525 NX Cryostat.
538 Immunofluorescence (IF) staining was performed following standard protocols [13]. Two
539 bleaching steps of 20 min each in 3% H_2O_2/MeOH were included for embryos or their tissues
540 carrying the Rosa26$^{mTmG/+}$ mutation in order to remove the tdTomato fluorescence [39].
541 Subsequently to completed IF, sections were coverslipped with Fluoro-Gel (with Tris buffer;
542 Electron Microscopy Sciences, USA), sealed and stored in the dark at 4°C.

543 *Whole tissues and embryos:* Whole tissues/embryos were fixed in 4% PFA for 60 minutes
544 on ice and stored in 0.0025% Triton X-100 (Sigma Aldrich) in PBS at 4°C until used.
545 Tissues/embryos were permeabilised using 0.25% Triton X-100 (PBS) for 60 minutes on
546 ice. IF staining was performed using previously published protocols [40-42]. E7.5 or E8.5 IF-
547 stained embryos were mounted on coverslips within SecureSeal imaging spacers (Grace
548 Bio-Labs) and embedded in RapiClear 1.52 solution (SUNJin Lab). Samples were stored in
549 the dark at 4°C before imaging.

550

551 **Microscopy**

552 *Epifluorescence microscopy:* IF sections were imaged on a Leica DM 2500 upright
553 microscope with a Leica DFC350 FX digital camera and a Leica EL6000 fluorescence light
554 source supported by the Leica Application Suite software package (LAS, version 3 or 4;
555 Leica Microsystems, Germany/Switzerland).

556 *Whole mount microscopy:* XGal-stained and GFP-positive embryos and tissues were
557 imaged using a Leica MZ 16F dissecting microscope equipped with a Leica DFC420 C
558 digital camera and a Leica EL6000 fluorescence light source supported by the LAS.

559 *Confocal microscopy:* Imaging of whole mount embryos was performed using an Andor
560 Dragonfly spinning disc confocal microscope (Andor, Oxford Instruments) mounted on an
561 inverted Leica DMi8 base using either a 10x (0.45NA) or a 25x water-dipping objective

562 (NA0.95). The z-steps for the 10x and 25x objectives were 1.32 µm and 0.35 µm,
563 respectively. DAPI, Alexa- 488, −568 and −647 were sequentially excited using 405nm 561,
564 637nm laser diodes, respectively, and emitted light reflected through 450/50 nm, 525/50nm,
565 600/50nm and 700/25nm bandpass filters, respectively. An iXon 888 EM-CCD camera was
566 used to collect emitted light, and data were captured using Fusion version 5.5 (Bitplane) with
567 subsequent image analysis performed using either Fiji [43] or Imaris (Bitplane). Images were
568 manually quantified by circling visible nuclei within a single z-plane to generate regions of
569 interest (ROI) using the ROI manager tool in FiJi. The average grey values were then
570 measured for the selected regions for each fluorescent channel.

571 *Light sheet microscopy:* The unfixed trunk area of E9.5 *Wt1*$^{CreERT2/+}$*; Rosa26*$^{mTmG/+}$ embryos
572 dosed with tamoxifen at E8.5, was mounted in 1% low melting point agarose (ROTI Garose,
573 Carl Roth, Karlsruhe, Germany), transferred into a capillary (Size 4, Brand GmbH,
574 Wertheim, Germany) and placed in the imaging chamber of a Zeiss Light Sheet Z.1
575 microscope with one 5x detection objective and two 5x illumination objectives supported
576 with the Zen software (Carl Zeiss, Jena, Germany). Imaging was performed using the 488
577 nm channel to capture GFP-positive cells, and the 561 nm channel to image membrane-
578 bound dTomato to provide tissue context. Images were adjusted to colours using the Imaris
579 software and the movie edited to highlight the shape of the selected area by using
580 the surface tool, and by labelling GFP-positive cells with coloured spots to indicate their
581 different locations.

582

583 **Analysis of single-cell mouse gastrulation atlas.**

584 Data analysis from a previously published dataset [21] was performed using R (version 4.3.2).
585 Data were accessed through Bioconductor 'MouseGastrulationData' package (version
586 1.16.0), and only processed data were extracted for downstream analysis. Extracted data
587 were normalised using *logNormCounts* function from 'scuttle' package (version 1.12.0).
588 Normalisation of cell count per sample was carried out by dividing total number of cells by
589 sample size and rounding up to the nearest integer. All plots were created using 'ggplot2'
590 package (version 3.4.3).

591

592 **4. References**

593

594 1 Donadon, M. & Santoro, M. M. The origin and mechanisms of smooth muscle cell
595 development in vertebrates. *Development* **148**, doi:10.1242/dev.197384 (2021).
596 2 Monte, G. d. *et al.* Differential Notch Signaling in the Epicardium Is Required for
597 Cardiac Inflow Development and Coronary Vessel Morphogenesis. *Circulation*
598 *Research* **108**, 824-836, doi:doi:10.1161/CIRCRESAHA.110.229062 (2011).
599 3 Qi, L., Kong, W., Fu, Y., Fu, X. & Xu, T. Vascular Smooth Muscle Cell Development
600 and Cardiovascular Malformations. *Cardiology Discovery* **01**, 259-268,
601 doi:doi:10.1097/CD9.0000000000000035 (2021).
602 4 Stratman, A. N. *et al.* Chemokine mediated signalling within arteries promotes
603 vascular smooth muscle cell recruitment. *Communications Biology* **3**, 734,
604 doi:10.1038/s42003-020-01462-7 (2020).
605 5 Hellstrom, M., Kalen, M., Lindahl, P., Abramsson, A. & Betsholtz, C. Role of PDGF-
606 B and PDGFR-beta in recruitment of vascular smooth muscle cells and pericytes
607 during embryonic blood vessel formation in the mouse. *Development* **126**, 3047-3055
608 (1999).
609 6 Smyth, L. C. D. *et al.* Markers for human brain pericytes and smooth muscle cells.
610 *Journal of Chemical Neuroanatomy* **92**, 48-60,
611 doi:https://doi.org/10.1016/j.jchemneu.2018.06.001 (2018).
612 7 Assinder, S. J., Stanton, J. A. & Prasad, P. D. Transgelin: an actin-binding protein
613 and tumour suppressor. *Int J Biochem Cell Biol* **41**, 482-486,
614 doi:10.1016/j.biocel.2008.02.011 (2009).
615 8 Armstrong, J. F., Pritchard-Jones, K., Bickmore, W. A., Hastie, N. D. & Bard, J. B.
616 The expression of the Wilms' tumour gene, WT1, in the developing mammalian
617 embryo. *Mech Dev* **40**, 85-97 (1993).
618 9 Kreidberg, J. A. *et al.* WT-1 is required for early kidney development. *Cell* **74**, 679-
619 691, doi:https://doi.org/10.1016/0092-8674(93)90515-R (1993).
620 10 Rackley, R. R. *et al.* Expression of the Wilms' tumor suppressor gene WT1 during
621 mouse embryogenesis. *Cell Growth Differ* **4**, 1023-1031 (1993).
622 11 Moore, A. W. *et al.* YAC transgenic analysis reveals Wilms' tumour 1 gene activity in
623 the proliferating coelomic epithelium, developing diaphragm and limb. *Mech Dev* **79**,
624 169-184 (1998).
625 12 Moore, A. W., McInnes, L., Kreidberg, J., Hastie, N. D. & Schedl, A. YAC
626 complementation shows a requirement for Wt1 in the development of epicardium,
627 adrenal gland and throughout nephrogenesis. *Development* **126**, 1845-1857,
628 doi:10.1242/dev.126.9.1845 (1999).
629 13 Wilm, B., Ipenberg, A., Hastie, N. D., Burch, J. B. E. & Bader, D. M. The serosal
630 mesothelium is a major source of smooth muscle cells of the gut vasculature.
631 *Development* **132**, 5317-5328, doi:10.1242/dev.02141 (2005).
632 14 Wilm, T. P. *et al.* Restricted differentiative capacity of Wt1-expressing peritoneal
633 mesothelium in postnatal and adult mice. *Scientific reports* **11**, 15940,
634 doi:10.1038/s41598-021-95380-1 (2021).
635 15 Que, J. *et al.* Mesothelium contributes to vascular smooth muscle and mesenchyme
636 during lung development. *Proc Natl Acad Sci U S A* **105**, 16626-16630,
637 doi:10.1073/pnas.0808649105 (2008).
638 16 Guadix, J. A., Carmona, R., Munoz-Chapuli, R. & Perez-Pomares, J. M. In vivo and
639 in vitro analysis of the vasculogenic potential of avian proepicardial and epicardial
640 cells. *Dev Dyn* **235**, 1014-1026, doi:10.1002/dvdy.20685 (2006).
641 17 Zhou, B. *et al.* Epicardial progenitors contribute to the cardiomyocyte lineage in the
642 developing heart. *Nature* **454**, 109-113, doi:10.1038/nature07060 (2008).

18 Carmona, R., Cano, E., Mattiotti, A., Gaztambide, J. & Munoz-Chapuli, R. Cells derived from the coelomic epithelium contribute to multiple gastrointestinal tissues in mouse embryos. *PloS one* **8**, e55890, doi:10.1371/journal.pone.0055890 (2013).

19 Chau, Y. Y. *et al.* Acute multiple organ failure in adult mice deleted for the developmental regulator Wt1. *PLoS Genet* **7**, e1002404, doi:10.1371/journal.pgen.1002404 (2011).

20 Hecksher-Sorensen, J. *et al.* The splanchnic mesodermal plate directs spleen and pancreatic laterality, and is regulated by Bapx1/Nkx3.2. *Development* **131**, 4665-4675, doi:10.1242/dev.01364 (2004).

21 Pijuan-Sala, B. *et al.* A single-cell molecular map of mouse gastrulation and early organogenesis. *Nature* **566**, 490-495, doi:10.1038/s41586-019-0933-9 (2019).

22 Richardson, L. *et al.* EMAGE mouse embryo spatial gene expression database: 2014 update. *Nucleic Acids Res* **42**, D835-844, doi:10.1093/nar/gkt1155 (2014).

23 Cano, E., Carmona, R. & Munoz-Chapuli, R. Wt1-expressing progenitors contribute to multiple tissues in the developing lung. *Am J Physiol Lung Cell Mol Physiol* **305**, L322-332, doi:10.1152/ajplung.00424.2012 (2013).

24 Dixit, R., Ai, X. & Fine, A. Derivation of lung mesenchymal lineages from the fetal mesothelium requires hedgehog signaling for mesothelial cell entry. *Development* **140**, 4398-4406, doi:10.1242/dev.098079 (2013).

25 Moiseenko, A. *et al.* Origin and characterization of alpha smooth muscle actin-positive cells during murine lung development. *Stem cells (Dayton, Ohio)* **35**, 1566-1578, doi:10.1002/stem.2615 (2017).

26 Rudat, C. & Kispert, A. Wt1 and epicardial fate mapping. *Circulation research* **111**, 165-169, doi:10.1161/CIRCRESAHA.112.273946 (2012).

27 Quijada, P., Trembley, M. A. & Small, E. M. The Role of the Epicardium During Heart Development and Repair. *Circulation research* **126**, 377-394, doi:10.1161/CIRCRESAHA.119.315857 (2020).

28 Nguyen, M. T., Zhu, J., Nakamura, E., Bao, X. & Mackem, S. Tamoxifen-dependent, inducible Hoxb6CreERT recombinase function in lateral plate and limb mesoderm, CNS isthmic organizer, posterior trunk neural crest, hindgut, and tailbud. *Dev Dyn* **238**, 467-474, doi:10.1002/dvdy.21846 (2009).

29 Zhu, J. *et al.* Uncoupling Sonic hedgehog control of pattern and expansion of the developing limb bud. *Developmental cell* **14**, 624-632, doi:10.1016/j.devcel.2008.01.008 (2008).

30 Funayama, N., Sato, Y., Matsumoto, K., Ogura, T. & Takahashi, Y. Coelom formation: binary decision of the lateral plate mesoderm is controlled by the ectoderm. *Development* **126**, 4129-4138, doi:10.1242/dev.126.18.4129 (1999).

31 Thomason, R. T., Bader, D. M. & Winters, N. I. Comprehensive timeline of mesodermal development in the quail small intestine. *Dev Dyn* **241**, 1678-1694, doi:10.1002/dvdy.23855 (2012).

32 Winters, N. I., Thomason, R. T. & Bader, D. M. Identification of a novel developmental mechanism in the generation of mesothelia. *Development* **139**, 2926-2934, doi:10.1242/dev.082396 (2012).

33 Prummel, K. D. *et al.* Hand2 delineates mesothelium progenitors and is reactivated in mesothelioma. *Nat Commun* **13**, 1677, doi:10.1038/s41467-022-29311-7 (2022).

34 Barnes, R. M., Firulli, B. A., Conway, S. J., Vincentz, J. W. & Firulli, A. B. Analysis of the Hand1 cell lineage reveals novel contributions to cardiovascular, neural crest, extra-embryonic, and lateral mesoderm derivatives. *Dev Dyn* **239**, 3086-3097, doi:10.1002/dvdy.22428 (2010).

35 Walton, K. D. *et al.* Villification in the mouse: Bmp signals control intestinal villus patterning. *Development* **143**, 427-436, doi:10.1242/dev.130112 (2016).

694 36 Hatch, J. & Mukouyama, Y. S. Spatiotemporal mapping of vascularization and
695 innervation in the fetal murine intestine. *Dev Dyn* **244**, 56-68, doi:10.1002/dvdy.24178
696 (2015).
697 37 Soriano, P. Generalized lacZ expression with the ROSA26 Cre reporter strain. *Nat*
698 *Genet* **21**, 70-71 (1999).
699 38 Muzumdar, M. D., Tasic, B., Miyamichi, K., Li, L. & Luo, L. A global double-fluorescent
700 Cre reporter mouse. *Genesis* **45**, 593-605, doi:10.1002/dvg.20335 (2007).
701 39 Lua, I., Li, Y., Pappoe, L. S. & Asahina, K. Myofibroblastic Conversion and
702 Regeneration of Mesothelial Cells in Peritoneal and Liver Fibrosis. *The American*
703 *journal of pathology* **185**, 3258-3273, doi:10.1016/j.ajpath.2015.08.009 (2015).
704 40 Baillie-Johnson, P., van den Brink, S. C., Balayo, T., Turner, D. A. & Martinez Arias,
705 A. Generation of Aggregates of Mouse Embryonic Stem Cells that Show Symmetry
706 Breaking, Polarization and Emergent Collective Behaviour In Vitro. *J Vis Exp*,
707 doi:10.3791/53252 (2015).
708 41 Beccari, L. *et al.* Multi-axial self-organization properties of mouse embryonic stem
709 cells into gastruloids. *Nature* **562**, 272-276, doi:10.1038/s41586-018-0578-0 (2018).
710 42 Turner, D. A. *et al.* Anteroposterior polarity and elongation in the absence of extra-
711 embryonic tissues and of spatially localised signalling in gastruloids: mammalian
712 embryonic organoids. *Development* **144**, 3894-3906, doi:10.1242/dev.150391
713 (2017).
714 43 Schindelin, J. *et al.* Fiji: an open-source platform for biological-image analysis. *Nat*
715 *Methods* **9**, 676-682, doi:10.1038/nmeth.2019 (2012).
716

717